Наносистеми, наноматеріали, нанотехнології
Nanosistemi, Nanomateriali, Nanotehnologii
2026, т. 24, № 1, сс. 141–163
https://doi.org/10.15407/nnn.24.01.0141

PACS numbers: 61.05.cp, 68.37.Hk, 68.43.Mn, 68.43.Pq, 68.47.Pe, 81.05.uj, 83.80.Mc

Study of Meloxicam Adsorption on Prepared Activated Nanocarbon from Pinecones: Thermodynamics and Kinetics

Lubna A. Al-Siqillee and Noha Mohammad Yahya

College of Education for Girls,
Department of Chemistry,
University of Mosul,
Mosul, Iraq

This research involves the preparation of activated nanocarbon using pinecones obtained from the forestry of the city of Mosul, Iraq. The prepared carbon is observed as nanoparticles with a particle size of 16.08 nm measured by a scanning electron microscope and a BET-theory surface area of 1.9719 nm^2. The iodine number of 1147 mg/g^{-1} and x-ray diffraction spectrum of the prepared activated carbon are also evaluated. The adsorption of meloxicam onto prepared activated carbon is studied in aqueous solutions. Freundlich and Langmuir isotherms are applied; the Freundlich model is more relevant to the practical data for the studied system due to the significant results of high $R^2 = 0.9968$ values compared to Langmuir's $R^2 = 0.9915$. The study of adsorption thermodynamically at equilibrium has shown that the adsorption process is spontaneous, as indicated by the negative value of Gibbs free energy (ΔG^0) and the low value of the entropy after the adsorption process (negative ΔS^0). Moreover, the type of adsorption refers to physical absorption ($\Delta H = -33.090$ kJ/mole) due to the force controlling the bond between the drug and the surface of carbon, which indicates adsorption as a heat-releasing process. Pseudo-first-order, pseudo-second-order, and intraparticle molecular diffusion are studied. The kinetic results show that the adsorption process at equilibrium follows the equation of a pseudo-second-order reaction, while interaction and molecular diffusion are not the only mechanisms dominating the adsorption process.

Це дослідження включало приготування активованого нановуглецю з використанням соснових шишок, отриманих з лісництва міста Мосул, Ірак. Підготовлене вугілля спостерігалося у вигляді наночастинок з розміром частинок у 16,08 нм, виміряним за допомогою сканувального електронного мікроскопа, та площею поверхні за Брунером, Емметом і Теллером (БЕТ-теорією) у 1,9719 $нм^2$. Також були оцінені йодне число 1147 $мг/г^{-1}$ та спектер рентґенівської дифракції підготовленого активованого вугілля. Адсорбцію мелоксикаму на підготовленому активова-

ному вугіллі вивчали у водних розчинах. Були застосовані ізотерми за Фрейндліхом і Ленґмюром; Фрейндліхів модель був більш релевантним для практичних даних стосовно досліджуваної системи завдяки значним результатам із високими значеннями $R^2 = 0{,}9968$ порівняно з $R^2 = 0{,}9915$ за Ленґмюром. Термодинамічне дослідження адсорбції в рівновазі показало, що процес адсорбції є спонтанним, на що вказує неґативне значення Ґіббсової вільної енергії (ΔG^0) та низьке значення ентропії після процесу адсорбції (неґативне ΔS^0). Більше того, тип адсорбції відноситься до фізичної абсорбції ($\Delta H = -33{,}090$ кДж/моль) через силу, яка контролює зв'язок між препаратом і поверхнею вуглецю, що вказує на те, що адсорбція є процесом виділення тепла. Була досліджена псевдопершого порядку, псевдодругого порядку та внутрішньочастинкова молекулярна дифузія. Кінетичні результати показують, що процес адсорбції в рівновазі відповідає рівнянню реакції псевдодругого порядку, хоча взаємодія та молекулярна дифузія є не єдиними механізмами, що домінують у процесі адсорбції.

Key words: pinecone, nanocarbon, surface area, Freundlich and Langmuir isotherms, adsorption, meloxicam, activated carbon.

Ключові слова: соснова шишка, нановуглець, площа поверхні, Фрейндліхові та Ленґмюрові ізотерми, адсорбція, мелоксикам, активоване вугілля.

(Received 25 July, 2024; in revised form, 5 September, 2024)

1. INTRODUCTION

The major problems of environmental pollution are one of the biggest facing the modern world and the most widespread due to industrial progress, which has caused an increase in the world's population. Industry is considered one of the biggest pollutants in the environment. Chemicals, or their biological decomposition products, are among the pollutants that affect the water ecosystem because they contain harmful chemical groups. Recently, pharmaceutical products have increased in their application, depending on their widespread use. As a result, large amounts of pharmaceutical products are discharged as waste materials, which cause the main environmental pollutants in liquids to be wasted due to their toxicity [1].

It is also considered an antibiotic-resistant pathogen. The classification of non-steroidal anti-inflammatory drugs (NSAIDs) represents one of the most important groups of pollutants due to their widespread use, as these medicines treat diseases that affect humans and animals in terms of their analgesic effect [2], anti-inflammatory effect, and antipyretic effect. In addition, NSAIDs belong to the OTC group of medications; without a prescription, they are the most common drugs observed in aqueous wastewater

because of their characteristics in terms of their hydrophobicity and stability [3].

NSAIDs can remain in the aqueous phases and can also exist at a surface concentration of up to 1 μg/L of water molecules [4]. The most common wastewater contamination is from homes, hospitals, clinics, or production plants. Medicine has prolonged exposure and caused bioaccumulation, which leads to chronic effects of toxicity that may include growth patterns, metabolism, and reproductive problems. The removal of NSAIDs has been applied in several ways, such as photocatalytic degradation [5, 6], microextraction [7], oxidation [8], biodegradation [9], chlorination [10], biofiltration [11], electrochemical oxidation [12] and an adsorption using activated carbon from different sources.

Meloxicam (MLX) is a member of NSAIDs has been observed in waste water in despite of its poor water solubility, its more soluble in alkaline solution at pH of 10.7 up to 19.9 mg/mL in recent study three type of activated carbon were synthesized and applied as sorbent for MLX removed sorbent for MLX removed from aqueous solution [1].

The aim of this study is to synthesized activated carbon from pinecone to be used for the removal of MLX from aqueous solution. This study includes the determination of adsorption efficiency and capacity of MLX in terms of isotherms, kinetics and thermodynamics at equilibrium.

Freundlich Isotherm. The Freundlich equation is one of the well-known isotherm models that can be successfully applied to single-component systems. This model assumes that the surface of the adsorbent is not homogeneous due to the irregularity of the potential energy on it as a result of the adsorption sites having varying levels of energy, the strength of the linear relationship can be expressed through the value of the correlation coefficient R^2, as this value is used to evaluate the extent, to which experimental data for adsorption can be represented by this isotherm. The linear model can be expressed as follows:

$$\log q_e = \log K_f + n^{-1} \log C_e, \tag{1}$$

where K_f and n represent Freundlich isotherm constants, the value of q_e represents the amount of adsorbed material per gram of adsorbent, which is known as the adsorption capacity (at equilibrium) (mg/g), while C_e represents the concentration of the remaining material, which is the non-adsorbed at equilibrium (mg/L). When drawing the relationship between $\log q_e$ *versus* $\log C_e$, it gives a straight line with a slope equal to $1/n$, which represents a measure of the intensity of adsorption, and a cross section equal to $\log K_f$,

which is a function of the adsorption capacity, whereas the value of n indicates the best value for obtaining the adsorbent feature and the degree of non-openness to the adsorbent feature layer, where, when it is only limited between 1–10, this means that adsorption is good and preferred; however, when the value of n is less than one, this adsorption is preferred and not preferable. When $n = 1$, this adsorption is linear, whereas when $n < 1$, the adsorption is chemical, and when $n > 1$, there is physical adsorption [13].

Langmuir Isotherm. This model assumes that molecules adsorb on a specific number of openings (pores) located on a specific weight of the adsorbent surface, which are energetically equivalent and each hole can hold only one adsorbed molecule, the molecules adsorbed on the adsorbent surface do not interfere with each other or with other attacking molecules present in the solutions. Therefore, a single layer of adsorbed molecules is formed on the adsorbent surface. According to this model, the adsorption phenomenon is rapid in the beginning and then reaches a state of equilibrium after the relative rate of speed equals due to the attachment of molecules on the surface of the adsorbent and the rate of their return to the solution [14]. According to this model, the amount of adsorbed material is proportional to the part exposed to the adsorption phenomenon, while the amount of returning particles is proportional to the covered part of the surface, this model can be expressed as follows:

$$C_e/q_e = 1/Q_{\max} + C_e/(bQ_{\max}), \tag{2}$$

where b is the Langmuir isotherm constant and indicates the strength of the drugs' attachment to the surface of the adsorbent material, while the value of $Q_{\max}$ represents the maximum theoretical capacity for adsorption of the adsorbent material (milligrams of adsorbent per gram of adsorbent material), while the values of C_e and q_e are the remaining concentration and adsorption capacity at equilibrium, respectively [15].

Kinetic Study. In order to obtain accurate information that explains the mechanism of adsorption and the kinetic forces affecting it, kinetic models were studied on the studied drug as follows.

The first description of the kinetic data for adsorption was by Lagergren, and that was through the pseudo-first-order equation, which is considered the first equation used to describe the speed rate of adsorption, based on its capacity, and then it was used by many researchers [16, 17]. The pseudo-first-order equation can be expressed as follows:

$$\ln(q_e - q_t) = \ln q_e - k_1 t. \tag{3}$$

In order for this model to apply to practical data for adsorption,

by plotting the relationship between $\ln(q_e - q_t)$ *versus* time t, it must give a linear relationship and a match must be obtained between the calculated and practical adsorption capacity value.

This model is also used to describe the kinetics of adsorption, as this model explains how the rate of speed depends on the adsorption capacity of the solid adsorbent and not on the concentration of the adsorbent. Unlike the other kinetic models, it predicts the behaviour of adsorption along the time period of adsorption, this is consistent with an adsorption mechanism that includes a step that determines the rate of speed, which may include countervailing forces through the sharing or exchange of electrons between the solution and the adsorbent, where the pseudo-second-order equation can be expressed as follows:

$$t/q_t = 1/\{k_2(q_e)^2\} + (1/q_e)t. \quad (4)$$

In order for this model to apply to practical adsorption data, by plotting the relationship between t/q_t *versus* time t, it must give a linear relationship, and a match must be obtained between the calculated and practical adsorption capacity value [16, 17]. It is also possible to use the adsorption rate constant k_2 to find the value of the initial pseudo-second-order adsorption speed (h) through Eq. (5):

$$h = k_2(q_{\text{ecal.}})^2. \quad (5)$$

The overall rate of adsorption will be determined by the slowest step, which may be diffusion from the outer boundaries of the liquid to the adsorbent surface, or the implicit molecular diffusion within the pores of the adsorbent material. The rate of adsorption speed on the active sites is assumed to be fast, and one of the important things that must be found and determined is the potential rate of speed specific to the adsorption mechanism. If the implicit molecular diffusion is the controlling factor, depending on the reaction rate, the process of removing adsorbed materials changes with the square root of time. As a result, it is possible to calculate the rate of adsorption speed by calculating the adsorption capacity of the adsorbent as a function of the square root of time, as the implicit molecular diffusion model can be represented by Eq. (6) [18]:

$$q_t = K_{diff}t^{1/2} + C; \quad (6)$$

K_{diff} ($\text{mg}\cdot\text{g}^{-1}\cdot\text{min}^{-1/2}$) represents the velocity rate constant for implicit molecular diffusion, while C ($\text{mg}\cdot\text{g}^{-1}$) is the value of the cross-section, and the value of K_{diff} can be found from the slope of the straight line.

2. EXPERIMENTAL METHOD

2.1. Instruments

Ultraviolet–Visible Spectrophotometer, double beam type (model 1800-UV) supplied by Shimadzu company, Japan. pH meter (Jenway 3510 model) was used for pH measurement. Scanning electron microscopy (SEM) was used to study the morphology. Oven and muffle furnace were used for drying and carbonization purposes, respectively. Water bath shaker of Type ST402 from Jwrio Tech. of Korean origin centrifuge used to isolate samples; the Hermle (LDZ4-2MEDICAL Low SPEED CENTERFUGE) type is of German origin and equipped by HERME LABORTECHNIK, SEM scanning device of MIRA3LMU model. The measurements were conducted at the University of Tabriz in Iran.

2.2. Chemical Materials

All chemical used, including hydrochloric acid (0.1M), potassium carbonate and distilled water supplied by BDH-Fluke company, thiosulphate, starch, iodine, meloxicam (MLX) 4-hydroxy-2-methyl-N-(5-methyl2-thiazolyl)-2H-1.2-benzothiazine-3-carboxamide-1,1-dioxide (Fig. 1) were supplied from Sammara drug company, Iraq. All solvents and reactants were at analytical grade.

Synthesized activated carbon (SAC), a new type of charcoal, was prepared using pine cone by cutting them, washing several times, drying under atmosphere air, and then, drying using oven at a temperature of 105–110°C for 48 hours, then, carry out the initial carbonization process by heating the powder at temperature of 450°C for 1:15 hour, then, the charcoal is cooled at room temperature, and for the purpose of performing the final carbonization, it is heated the charcoal powder using muffle furnace after mixing it with (K_2CO_3) in ratio of (1:1) by weight of (K_2CO_3:charcoal) to a degree of temperature of 750°C for one hour. Then, the mixture was cooled and washed with distilled water several times until the pH of

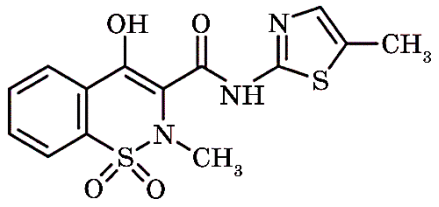

Fig. 1. Structural formula of meloxicam.

the washing water was equal to 7. Then, it was treated with a solution of 5% hydrochloric acid and heated for two hours. Then, it is cooled to laboratory temperature and washed until the acidity of the wash water reaches = 7. The prepared activated charcoal was dried well, then, mechanically crushed, and molecular sieves were used to isolate it and preserved in sealed containers for subsequent study.

2.3. Adsorption

Many factors may be affected on the adsorption efficiency and adsorption capacity like the amount of activated carbon, initial concentration of MLX, contact time, temperature and pH were studied to investigate the optimum condition of these parameters.
Determination of the Iodine Number of SAC. The adsorption of iodine was reported in a simplest test for determination of surface area of a synthesized activated carbon (SAC), which correlated to the volume of pores. Iodine number was considered as the amount of iodine solution per 0.25 mg of activated carbon placed in 250 mL of conical flask, then, added 5 mL of cone HCl and boiling for 30 sec. After cooled, the sowing 25 mL of iodine solution (0.1 N) were added and shaken for 10 min. The suppurated was filtrated; 5 mL of filtrate was calibrated with sodium thiosulphate (0.1 N) using addition of two drops of starch. Iodine number (1. N) was calculated as

$$IN = \frac{5\left(10C_1 - 1.2C_2V_2\right)126.93D}{m}, \tag{7}$$

where C_1 [mole·L^{-1}] refers to the concentration of standard iodine solution; C_2 [mole·L^{-1}] represents the concentration; V_2 [mL] volume of burette; m [gm] weight of coal; D is the correction factor.

2.4. Determination of the Amount of Adsorbent

Both the adsorption efficiency and capacity are used to express the amount of the adsorbed substance, by estimating the remaining amount of the substance in the solution. Since the drug that was studied is not coloured, the spectroscopic method in the (UV) region, which falls in the lower range 362 nm, was calculated. The amount of adsorbed material is determined by the difference between the initial concentration and the remaining concentration in the solution. The calibration curve was adopted to find these concentrations. The adsorbed material, adsorption efficiency, and adsorption capacity were found using Eq. (8), (9):

$$A = \varepsilon bCl, \tag{8}$$

$$q_e = (C_i - C_e)V_L/m\,, \tag{9}$$

$$\text{Adsorption [\%]} = \{(C_i - C_e)/C_i\} \cdot 100\,, \tag{10}$$

where A represents the absorption, ε is the absorption coefficient, b is length of the light path for visible rays, C is the concentration, l represents the cell width ($l = 1$ cm), C_i represents the initial concentration, C_e represents the remaining concentration, $(C_e - C_i)$ represents the adsorbed concentration, which is symbolized by C_{ads}, while q_e represents the adsorption capacity, as for V_l is the volume of the drug solution in [litres], and m is the weight of the adsorbed material [g]. All concentrations are in [mg/L].

2.5. The Use of the Batch Method

All studies have been completed on the influence of factors on the adsorption process and its kinetic studies, which include applying the study in a one-shot method by changing some variables and fixing others, as follows.

Solutions of different concentrations of the drug were prepared in tightly sealed conical glass flasks under the same conditions. Then, quantities of adsorbent material prepared activated carbon were added to it, and it was shaken continuously at specific times and at a rate of shaking (100 revolutions/minute) using a water bath shaker after with temperature controller [19].

3. RESULTS AND DISCUSSION

3.1. Adsorbent Material

The surface of the material was characterized using an experimental study with Debye–Scherrer Eq. (11) [20]:

$$D = k\lambda/(\beta\cos\theta), \tag{11}$$

where D—the size of minutes in aggregate unit, k—Debye's constant equal to 0.94, λ—the total wavelength of 1.5406 Å copper, β—the total width at the maximum opening of the apex. The full width at half-maximum $FWHM$ is measured in the degree unit [deg.] and converted to the unit [rad]), as the $FWHM$ value is set by π/180, and θ is the diffraction angle in [deg.] (Fig. 2).

The x-ray spectrum notes the presence of several bands, each band indicating a specific phase. The bands located at the location ($2\theta = 23°$) and ($2\theta = 43°$) belong to the (100) and (002) phases, respectively, which confirm the natural porous structure of activated

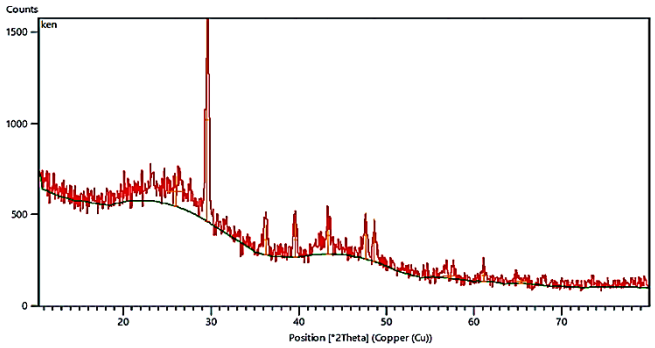

Fig. 2. X-ray diffraction (XRD) spectrum of prepared activated charcoal.

carbon. In addition, the presence of this broad band in the spectrum of activated carbon indicates that the carbon has a high surface area, and these results were consistent with the values of the surface area and the microscopic image of the scanning electron device, which showed that activated carbon possesses structural porosity [21].

From the high-field scanning electron microscope images shown at different magnification powers, the carbon surface has porous as it contained a large number of pores in different shapes and sizes. It was also noted that there were white crystals on the surface of the activated carbon, which play an essential role in the process of removing pollutants from the liquid phase, as shown in Fig. 3.

3.2. Determine the Maximum Wavelength and Calibration Curve

The maximum wavelength λ_{max} was determined at the highest absorption of the solution prepared from the drug under study, by recording the absorption spectrum of the drug solution with an appropriate concentration, through which the highest wavelength of the drug solution was determined. Different concentrations of drug solution were prepared from stock solution 1000 ppm, then, the absorption of the solution at those concentrations was detected to plot the relationship between the absorption with the corresponding concentrations by applying the Beer–Lambert law. It was found that the λ_{max} value of MLX is of 362 nm, as shown in Fig. 4.

3.3. The Effect of Adsorbent Weight

This study was conducted for a series of solutions of 25 mL with concentrations of the drug meloxicam at 35 ppm with different

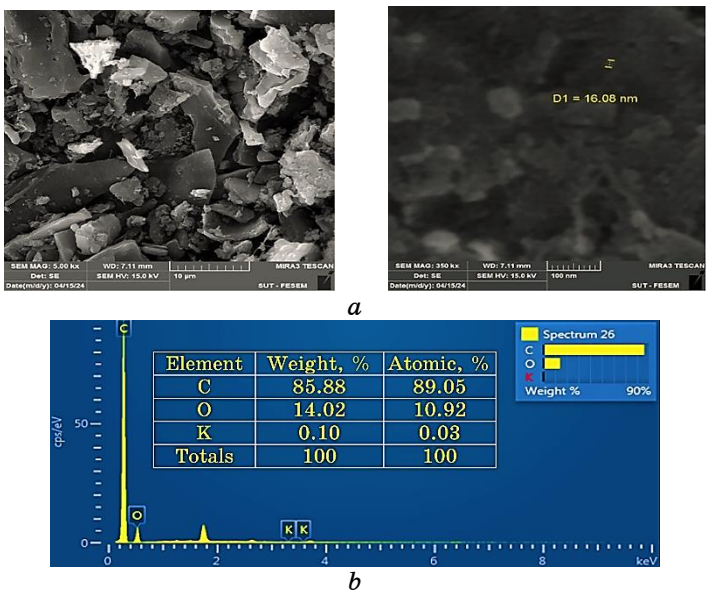

Fig. 3. *a*—SEM; *b*—XRD shapes of the surface of prepared carbon (SAC).

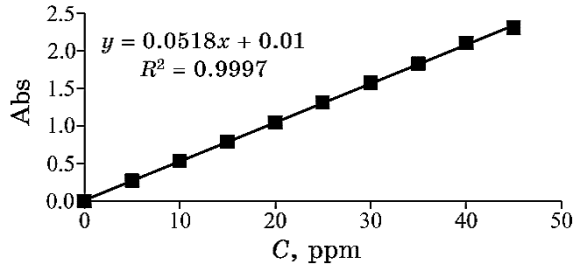

Fig. 4. Calibration curve for the MLX.

weights of activated charcoal prepared to obtain the required removal ranging from 0.01 g to 0.12 g. After shaking these solutions for a period of 60 minutes, the solutions were separated and the absorption was measured and calculated. The concentrations of the remaining materials were then estimated, and the adsorption capacity and percentage of adsorption were estimated based on Eq. (1) and Eq. (2), respectively. Studying the effect of the amount of adsorbent material is considered very important because it has a significant impact on the adsorption process, and those weights mentioned were adopted in our current study [22], as in the following Table 1.

The adsorption capacity decreases with an increase in the weight of the adsorbent, accompanied by an increase in the percentage of

TABLE 1. Effect of the amount of adsorbent in the efficiency and capacity of adsorption for 60 min. at 25°C; shaking speed of 100 rpm; a concentration of 35 ppm of 25 mL of MLX drug solution.

Type of adsorbent	C_i, mg/L	Quantity of adsorbent, g	C_e, mg/L	%	q_e, mg/L
SAC	35	0.01	21.467	38.665	33.832
		0.02	20.405	41.699	18.243
		0.04	13.320	61.941	13.549
		0.06	9.131	73.910	10.778
		0.08	6.833	80.474	8.801
		0.1	4.305	87.699	7.673
		0.12	2.278	93.491	6.817

TABLE 2. The effect of concentration in the efficiency and capacity of adsorption for 60 min.; the amount of adsorbent is of 0.12 g at 25°C; shaking speed of 100 rpm of 25 mL of MLX solution.

Type of adsorbent	C_i, mg/L	C_e, mg/L	%	q_e, mg/g
SAC	15	0.424	97.168	3.036
	20	0.965	95.173	3.965
	25	1.312	94.749	4.934
	30	2.007	93.307	5.831
	35	2.277	93.491	6.817
	40	4.729	88.175	7.347
	45	6.196	86.229	8.083
	50	7.760	84.478	8.798
	55	9.961	81.888	9.383

adsorption. This can be explained by the fact that increasing the amount of adsorbent increases the number of empty effective adsorption sites [23], which leads to a decrease in the adsorption capacity when a specific number of drug molecules are adsorbed using fixed concentrations of meloxicam, and at the same time the percentage of adsorption increases. With the increase in the amount of adsorbent material, this is due to the easily attachment between the drug molecules and the sites eligible for adsorption on the surface of the adsorbent material.

3.4. The Effect of Initial Concentration

The results obtained with studying the effect of the initial concen-

tration are shown in Table 2.

The results in Table 2 is a sequential adsorption reduction with increasing concentration and for all adsorbed materials, because increasing concentrations at the beginning of adsorption lead to an increase in the number of available molecules over time as they compete among molecule by molecule in association to achieve distinction of sites, and the continuity remaining on the surface of the adsorbent was with a constant quantity that is likely to be used with increasing the concentration leading to the occurrence of a larger amount of adsorbent in the solutions. Thus, an increase in the remaining amount in the solutions is greater with increasing concentrations in working on an effective rate of adsorption (an effective rate of adsorption), while the safety of adsorption increases with increasing concentrations due to the increase in concentrations. In the adsorbent material, small quantities are recorded [24].

3.5. Effect of Contact Time

The effects of contact time shown in Table 3.

These results obtained in the Table 3 regarding the effect of contact time indicate that the adsorption process in the beginning, from the first minutes, is very fast, and then it begins to slow down gradually until the adsorption is reached to a state of equilibrium, since the adsorption process takes place after the equilibrium occurs, it remains approximately constant, since the adsorption process reaches the speed, at which the molecules of the adsorbent (drug) bond to the surface of the adsorbent, equal to the speed of the return of other molecules from the adsorbent surface to the solution. This is called as the state of equilibrium. It has been found

TABLE 3. Effect of contact time in the efficiency and capacity of adsorption at 25°C; the amount of charcoal prepared of 0.12 g; an initial concentration of 35 ppm for MLX solution.

Type of adsorbent	Time, min.	C_e, mg/L	%	q_t, mg/g
SAC	10	8.977	74.351	5.421
	20	8.745	75.013	5.469
	30	7.568	78.378	5.715
	40	5.927	83.066	6.056
	50	4.730	86.486	6.306
	60	2.277	93.491	6.817
	70	2.239	93.601	6.825
	80	2.239	93.601	6.825

that all materials under study have reached to equilibrium in a time ranging between 60–70 min.; this variation in the speed of adsorption occurs due to the abundance of empty active sites that are found on the surface of the adsorbent material, which qualifies it to bind to the adsorbent material at the beginning of the adsorption process, in addition to the fact that the concentration of the adsorbent material at the beginning of adsorption is high, which easily accomplishes the process of transferring the molecules of the adsorbent material (meloxicam) to the surface of the adsorbent material (SAC), and with the passage of time it will decrease at the effective eligible sites for adsorption, and with it, the competition between the drug molecules to bind to these eligible sites will increase, resulting in a decrease in the acceleration of the adsorption process until the system reaches a state of equilibrium [25].

3.6. Effect of Temperature

The effect of temperature on the adsorption of drugs adsorbed on the surface of activated charcoal was studied over a specific range of temperatures ranging from 288–338 K, as the effect of temperature is considered one of the important studies for calculating the thermodynamic functions ΔS^0, ΔH^0, and ΔG^0. This study was conducted at fixed concentrations of the drug and fixing all other variables, including the amount of adsorbent and the natural acid value of meloxicam, and using a fixed volume of the drug solution 25 mL and a constant shaking speed of 100 revolutions/minute. Table 4 shows the results obtained.

According to the results listed in Table 4, an increase in temperature leads to a decrease in the adsorption efficiency (percentage) and the adsorption capacity in all materials under study. This means that increasing the temperature will lead to an increase in the process of the return of the molecules of the adsorbed material

TABLE 4. Effect of temperature in the efficiency and capacity of adsorption using the amount of adsorbent 0.12 g; an initial concentration of 35 ppm; a time of 70 minutes.

Type of adsorbent	Temperature, K	C_e, mg/L	%	q_e, mg/g
SAC	288	1.428	95.918	6.994
	298	2.239	93.601	6.825
	308	3.861	88.968	6.487
	318	5.250	84.997	6.197
	328	7.297	79.150	5.771
	338	8.146	76.723	5.594

from the surface of the adsorbent to the solution. This is as a result of the breaking of the bonding forces between the adsorbent material and the adsorbent surface, and this indicates that the adsorption process is heat-emitting, which clearly indicates the physical nature of adsorption in the carefully studied system, and that this statement is completely consistent with the rule of Chatelier [26].

3.7. pH Effect

The results obtained of studying the effect of acid function are shown in Table 5.

The natural acid function of drugs is shown with the symbol (*), which is indicated on the number of the natural acid function for each drug shown, and from Table 5. It has been observed that the adsorption efficiency and adsorption capacity decrease clearly when moving with the acid function from the acidic medium to the neutral medium and then the basic medium. It is concluded that the process adsorption may occur in acidic and basic functions. It is known that the surface of activated carbon is dominated by a negative charge and a small amount of positive charge. In the acidic medium, the proton atoms dominate the solution, which is equivalent to the positive charge on the surface. However, in the basic medium, it is dominated by the negative charge, as these charges are equivalent to the positive charge in the drug compound, thus hindering its movement. It reduces the adsorption efficiency [27].

3.8. Calculating Thermodynamic Parameters

Thermodynamic functions are among the important variables that give a distinct interpretation when studying the adsorption process.

TABLE 5. Effect of acid function in the efficiency and capacity of adsorption at a time of 70 min.; an initial concentration of 35 ppm at 25°C; the amount of adsorbent material is of 0.12 g; a shaking speed of 100 rpm of 25 mL of MLX solution.

Type of adsorbent	pH	C_e, mg/L	C_{ads}, mg/L	%	q_e, mg/g
SAC	13	1.525	33.474	95.642	6.973
	12*	2.239	32.760	93.601	6.825
	11	3.513	31.486	89.961	6.559
	10	4.710	30.289	86.541	6.310
	9	5.463	29.536	84.390	6.153
	8	6.911	28.088	80.253	5.851

They explain the nature of the system studied, as well as the type of forces that control it and the course of the adsorption process. In addition, they can give an idea of the type of molecular interactions that can occur during the adsorption process, which have a major role in determining its competence. The heat of adsorption can be found from the Van't Hoff equation, which represents the relationship between temperature and the equilibrium constant:

$$K_c = K_0 e^{-\Delta H/RT}, \tag{12}$$

where ΔH represents the heat of adsorption, K represents the equilibrium constant for adsorption, while K_0 represents a constant value.

Taking ln for both sides, we get the following form:

$$\ln K_c = \ln K_0 \cdot \{-\Delta H/(RT)\}, \tag{13}$$

The value of ΔH can be found by drawing the relationship between ln$K$ *versus* the reciprocal of temperature $1/T$, which gives a straight line with a slope equal to $(-\Delta H/R)$, and by knowing the value of the equilibrium constant for adsorption, which can be found from the ratio between concentration of the adsorbed material remaining in the solution:

$$K_c = C_{ads}[\text{mg/L}]/C_e[\text{mg/L}]. \tag{14}$$

It is possible to find the value of ΔH and then find the other thermodynamic functions ΔS^0, ΔG^0 through the following equations:

$$\Delta G^0 = -RT\ln K_c, \tag{15}$$

$$\Delta G^0 = \Delta H - T\Delta S^0, \tag{16}$$

$$\Delta S^0 = (\Delta H - \Delta G^0)/T. \tag{17}$$

The value of ΔG^0 represents the change in the standard free energy at any stage of adsorption, while ΔG^0 represents the zero value and the free energy, when the equilibrium process is constant. Therefore, the value of ΔS^0 was found, which represents the state of the system at any stage of adsorption stages [28].

As for the figure that represents the linear relationship resulting from plotting ln$K$ *versus* $1/T$ by applying the Van't Hoff Eq. (12), it is shown in Fig. 5 and Table 6.

The values of the equilibrium constants K_c decrease with increasing temperature for a single drug, which agrees with what was previously found, as the efficiency of adsorption decreases with in-

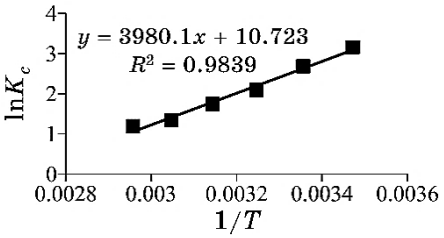

Fig. 5. The relationship between $\ln K_c$ *versus* $1/T$ to calculate the thermodynamic functions for drug adsorption.

TABLE 6. Equilibrium constants and thermodynamic functions at equilibrium.

Type of adsorbent	Temperature, K	K_c	ΔG, kJ·mole^{-1}	ΔH, kJ·mole^{-1}	ΔS, J·mole^{-1}·K^{-1}
SAC	288	23.5	–7.559	–33.090	–88.605
	298	14.629	–6.647		–88.735
	308	8.065	–5.345		–90.081
	318	5.665	–4.585		–89.638
	328	3.796	–3.637		–89.794
	338	3.296	–3.351		–87.984

creasing temperature, which indicates that the forces responsible for the adsorption process are physical forces, as the increase in temperature leads to its breakdown. Then, the adsorbed molecules return to the solution.

The value of the enthalpy change ΔH that was calculated over a range of temperatures, in which Van't Hoff assumed that the value of (ΔH) is constant over a certain range of temperatures, was all of a negative sign, which indicates that the adsorption process is heat emitting. While their values indicate the type and nature of the forces responsible for the adsorption process, they are of a physical nature, as all their obtained values are less than 40 kJ·mole^{-1}, which is within the energy range of physical bonds [25]. Most of the forces in which drugs bind to the adsorbent surface (carbon) are of the type of hydrogen bonding forces, whose energy ranges 5–15 kJ/mole.

The negative values of ΔS^0 give an indication of the state of regularity in the system studied. What is worth noting is that the strength of the interference and the preference for adsorption to occur over extortion and the fact that its values are within a certain range and are close at all temperatures, this supports that the system is of a physical nature, and that the role of entropy change

is limited. In influencing the progress of the adsorption process, these results are supported by the values of the change in free energy ΔS^0, as their values indicate a decrease in the spontaneity of adsorption with the increase in temperature.

3.9. ADSORPTION ISOTHERMS

3.9.1. Freundlich Isotherm

When applying Eq. (1) for this isotherm to the practical data for adsorption, by drawing the graphical relationship between $\log q_e$ *versus* $\log C_e$, and through it, the values of the Freundlich constants K_f, n were calculated from the slope n and the cross-section K_f of the straight line in order, as shown in Fig. 6 and Table 7.

As observed, the results listed in Table 7 showed that the Freundlich isotherm equation applied to the data for the adsorption system was fitted based on the data of correlation coefficient value $R^2 = 0.9968$, so that isotherm Freundlich is more applicable to describe the adsorption of MLX. Therefore, the adsorption followed a multilayer model as a heterogeneous surface indicated by n value of 3.203, which is between 1 and 10. Moreover, the adsorption process is higher than desorption process for the value of K_f, which has a relationship with the adsorption coupling, with energy value and a factor that depends on the nature of both the adsorbent and the adsorbent [30].

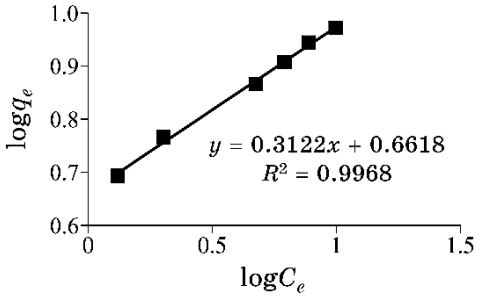

Fig. 6. Application of Freundlich isotherm to practical data for adsorption of the studied drug.

TABLE 7. Freundlich constants K_F, n and correlation coefficient R^2 obtained by applying them to practical adsorption data.

Type of adsorbent	Drug	n	K_f	R^2
SAC	meloxicam	3.203	4.589	0.9968

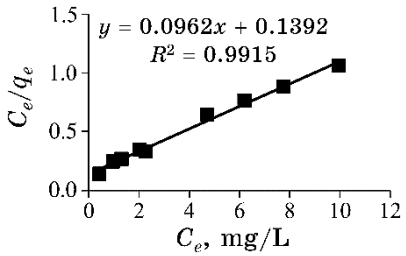

Fig. 7. Application of the Langmuir isotherm to experimental drug adsorption data.

TABLE 8. Langmuir constants b, Q_{max} and the correlation coefficient R^2 obtained by applying them to practical adsorption data.

Type of adsorbent	Drug	Q_{max}, mg/g	K_L, L/mg	R^2
SAC	meloxicam	10.395	0.691	0.9915

3.9.2. Langmuir Isotherm

This isotherm is the most common and applied to practical adsorption data. Through it, information is obtained that shows the extent of the ability of the adsorbent material to absorb molecules of the adsorbent material, which is represented by the maximum theoretical adsorption capacity Q_{max} [mg/g], which is supposed to be in the form of a single layer on the surface. The strength of its connection is also expressed by the Langmuir constant K_L [L/mg].

The practical results of the adsorption of the drugs, which were chosen to complete this study, were applied to the surface of the adsorbent materials at equilibrium using the mathematical equation of the Langmuir isotherm, Eq. (2), by drawing the graphical relationship between C_e/q_e *versus* C_e, and the Langmuir constants Q_{max} and K_L were calculated from the slope and cross-section of that straight line, as shown in Fig. 7 and Table 8.

3.10. KINETICS STUDY

3.10.1. Pseudo-First Order Equation

The pseudo-first order equation model, Eq. (3), was applied by drawing the relationship between $\ln(q_e - q_t)$ *versus* t (the time per minute) to obtain a linear relationship with the magnitude of its slope k_1 and its intercept $\ln q_e$ and through it, values of q_e and k_1 can be found. The shape and results obtained are shown in Fig. 8 and

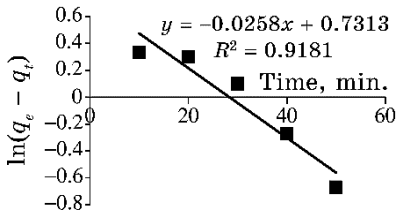

Fig. 8. Pseudo-first order model to experimental drug adsorption data.

TABLE 9. Practical and theoretical pseudo-first-order rate constants, adsorption capacity, and the correlation coefficient obtained by applying them to practical adsorption data.

Type of adsorbent	Drug	$q_{e(exp)}$, mg/g	$q_{e(calc.)}$, mg/g	K_1, min.$^{-1}$	R^2
SAC	meloxicam	6.825	2.077	0.0258	0.9181

listed in Table 9.

3.10.2. Pseudo-Second Order Equation

When applying the pseudo-second order model to practical adsorption data by plotting the relationship between t/q_t *versus* time t as Eq. (4), it is also possible to use the adsorption rate constant k_2 to find the value of the initial pseudo-second-order adsorption speed h through Eq. (5). The shape and results obtained are shown in Fig. 9 and listed in Table 10.

3.10.3. Intraparticle Diffusion Model

The intraparticle diffusion model was applied to the practical data for adsorption by applying Eq. (6) by plotting the relationship between the value of q_t *versus* the square root of time. The value of C gives evidence of the thickness of the outer layer of the solution boundaries and its effect, as a high value of C indicates this class as having a greater influence. The shape and results obtained are shown in Fig. 10 and listed in Table 11.

According to the results presented in Table 11 and from the shapes shown in Fig. 10, the implicit molecular diffusion mechanism will be the only mechanism that guides the adsorption process, only when the relationship between q_t *versus* $t^{1/2}$ is blinded by a straight line passing through the original point, and since this does not happen, it is inferred that the process of implicit molecular diffusion plays an important role in the process of removing the drug

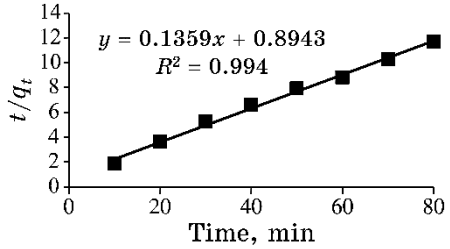

Fig. 9. Application of the pseudo-second order model to experimental drug adsorption data.

TABLE 10. Rate constant of practical and theoretical pseudo-second order adsorption capacity and correlation coefficient obtained by applying them to practical adsorption data.

Type of adsorbent	Drug	$q_{e(exp)}$, mg/g	$q_{e(calc.)}$, mg/g	K_2, g·mg^1·min.$^{-1}$	h, mg·g^{-1}·min^{-1}	R^2
SAC	meloxicam	6.825	7.358	0.0206	0.962	0.994

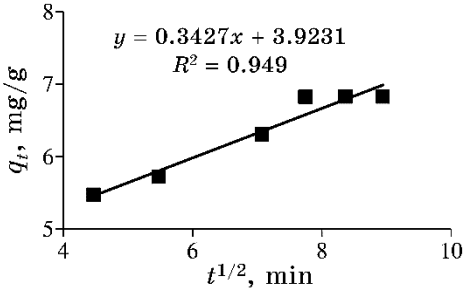

Fig. 10. Application of the intraparticle molecular diffusion model to practical drug adsorption data.

TABLE 11. Intramolecular diffusion constants and correlation coefficient obtained from their application to practical adsorption data.

Type of adsorbent	Drug	C_i, mg/L	K_{diff}, mg·g^{-1}·min$^{-1/2}$	C, mg·g^{-1}	R^2
SAC	meloxicam	35	0.3427	3.9231	0.949

from its aqueous solutions using activated carbon.

With the experimental results, it suggested that not the only mechanism controlling the drug adsorption as shown previously. The results listed in Table 11 have shown that an increase in drug concentration leads to increase, in the force for adsorption, in the

drug diffusion rate K_{diff}. It has been observed that increasing of the drug concentration leads to an increase in the thickness of the boundary layer between the carbon surface and the drug molecules [31].

4. CONCLUSIONS

As concluded, a novel activated nanocarbon was prepared from pinecone and then characterized. The nanoparticles of activated carbon were applied to study the adsorption of MLX from its aqueous solution. The optimum condition of the adsorption process was evaluated, such as the amount of adsorbent in SAC of 0.12 g with the initial concentration of MLX of 15–35 mg/L for 60 minutes of contact time at equilibrium for alkaline medium at 288–338 K, and the adsorption was found to be an exothermic process. The experimental process of adsorption was evaluated using the Langmuir and Freundlich isotherms to detect the type of adsorption. Based on the correlation ($R^2 = 0.996$), the Freundlich model has a significant pattern compared to other models, which were fitted to the experimental data. Hence, the adsorption process is suggested to be a heterogeneous, multilayer process. Kinetically, the adsorption process is followed by a pseudo-second-order reaction.

ACKNOWLEDGEMENTS

Authors would like to thank the University of Mosul, College of Education for Girls, Chemistry Department, management and staff for all the support during the experimental work stage.

REFERENCES

1. Masoumeh Mohammadnejad and Alieh Moeinipour, *Analytical and Bioanalytical Chemistry Research*, **11**, Iss. 1: 77 (2024); https://doi.org/10.22036/abcr.2023.409114.1962
2. S. H. Huo, H. Y. An, J. Yu, X. F. Mao, Z. Zhang, L. Bai, and P. X. Zhou, *Journal of Chromatography A*, **1517**: 18 (2017); https://doi.org/10.1016/j.chroma.2017.08.039
3. Y. Bian, N. Xiong, and G. Zhu, *Processes*, **6**, Iss. 8: 122 (2018); https://doi.org/10.3390/pr6080122
4. J. R. de Andrade, M. F. Oliveira, M. G. da Silva, and M. G. Vieira, *Industrial & Engineering Chemistry Research*, **57**, Iss. 9: 3103 (2018); https://doi.org/10.1021/acs.iecr.7b05137
5. S. Pap, M. A. Taggart, L. Shearer, Y. Li, S. Radovic, and M. T. Sekulic, *Chemosphere*, **264**: 128439 (2021); https://doi.org/10.1016/j.chemosphere.2020.128439

6. S. Banerjee and F. Maric, *European Journal of Physiotherapy*, **25**, Iss. 1: 51 (2023); https://doi.org/10.1080/21679169.2021.1976272
7. H. Lord and J. Pawliszyn, *Journal of Chromatography A*, **902**, Iss. 1: 17 (2000); https://doi.org/10.1016/S0021-9673(00)00836-0
8. G. R. Wallwork, *Reports on Progress in Physics*, **39**, Iss. 5: 401 (1976); doi:10.1088/0034-4885/39/5/001
9. A. Sivan, *Current Opinion in Biotechnology*, **22**, Iss. 3: 422 (2011); https://doi.org/10.1016/j.copbio.2011.01.013
10. C. Noutsopoulos, E. Koumaki, D. Mamais, M. C. Nika, A. A. Bletsou, and N. S. Thomaidis, *Chemosphere*, **119**: S109 (2015); https://doi.org/10.1016/j.chemosphere.2014.04.107
11. A. Binelli, S. Magni, C. Soave, F. Marazzi, E. Zuccato, S. Castiglioni, M. Parolini, and V. Mezzanotte, *Ecological Engineering*, **71**: 710 (2014); https://doi.org/10.1016/j.ecoleng.2014.08.004
12. R. F. B. De Souza, L. S. Parreira, D. C. Rascio, J. C. M. Silva, E. Teixeira-Neto, M. L. Calegaro, E. V. Spinace, A. O. Neto, and M. C. Santos, *Journal of Power Sources*, **195**, Iss. 6: 1589 (2010); http://dx.doi.org/10.1016/j.jpowsour.2009.09.065
13. A. L. Myers and P. A. Monson, *Adsorption*, **20**: 591 (2014); https://doi.org/10.1007/s10450-014-9604-1
14. E. A. Al-hyali, T. Ra'ed, and N. H. Saleem, *Samarra Journal of Pure and Applied Science*, **3**, Iss. 4: 41 (2021); https://doi.org/10.54153/sjpas.2021.v3i4.292
15. J. Wang and X. Guo, *Chemosphere*, **258**: 127279 (2020); https://doi.org/10.1016/j.chemosphere.2020.127279
16. Fadirah Fadzail, Masitah Hasan, and Zulfakar Mokhtar, *IOP Conf. Ser.: Earth Environ. Sci.*, **646**, No. 1: 012031 (2012); doi:10.1088/1755-1315/646/1/012031
17. A. M. Ali, R. Alsaqa, and N. S. Sultan, *International Journal of Thermodynamics*, **25**, Iss. 2: 33 (2022); https://doi.org/10.5541/ijot.1003950
18. K. Chinoune, K. Bentaleb, Z. Bouberka, A. Nadim, and U. Maschke, *Applied Clay Science*, **123**: 64 (2016); https://doi.org/10.1016/j.clay.2016.01.006
19. C. Nanthamathee and P. Dechatiwongse, *Materials Chemistry and Physics*, **258**: 123924 (2021); https://doi.org/10.1016/j.matchemphys.2020.123924
20. D. Mohammadyani, S. A. Hosseini, and S. K. Sadrnezhaad, *International Journal of Modern Physics: Conference Series*, **5**: 270 (2012); https://doi.org/10.1142/S2010194512002127
21. Q. M. Abdulhamid, E. T. Al-Tikrity, A. B. Fadhil, and P. J. Foot, *Journal of Analytical and Applied Pyrolysis*, **173**: 106072 (2023); https://doi.org/10.1016/j.jaap.2023.106072
22. H. Tun and C. C. Chen, *Adsorption*, **27**, Iss. 6: 979 (2021); https://doi.org/10.1007/s10450-020-00296-3
23. R. S. Abdul Hamza, I. Oreibi, and M. A. Habeeb, *Nanosistemi, Nanomateriali, Nanotehnologii*, **22**, Iss. 2: 379 (2024); https://doi.org/10.15407/nnn.22.02.379
24. K. Y. Foo and B. H. Hameed, *Chemical Engineering Journal*, **166**, Iss. 2: 792 (2011); https://doi.org/10.1016/j.cej.2010.11.019
25. M. Abdulkarim, I. L. Ibrahim, M. Mohammed, and M. Musah, *Fudma Journal of Sciences*, **8**, Iss. 3: 409 (2024); https://doi.org/10.33003/fjs-2024-

0803-2567
26. Y. Ngernyen, D. Petsri, K. Sribanthao, K. Kongpennit, P. Pinijnam, R. Pedsakul, and A. J. Hunt, *RSC Advances*, **13**, Iss. 21: 14712 (2023); https://doi.org/10.1039/D3RA01949G
27. S. F. Fatima, R. Sabouni, G. Husseini, V. Paul, H. Gomaa, and R. Radha, *Nanomaterials*, **14**, Iss. 13: 1081 (2024); https://doi.org/10.3390/nano14131081
28. S. Sivalingam and S. Sen, *Environ. Sci. Pollut. Res.*, **26**: 34693 (2019); https://doi.org/10.1007/s11356-018-3664-9
29. K. A. AL-Memary, E. A. Al-Hyali, and H. T. A. S. Toohi, *Research Journal of Pharmacy and Technology*, **12**, Iss. 3: 1206 (2019); http://dx.doi.org/10.5958/0974-360X.2019.00201.4
30. L. Z. Zhang and L. Wang, *Applied Thermal Engineering*, **19**, Iss. 2: 195 (1999); https://doi.org/10.1016/S1359-4311(98)00023-4
31. E. A. S. Al-Hyali, K. A. O. AL-Memary, and T. AL-Sayd, *Journal of Education and Science*, **29**, No. 1: 233 (2020); doi:10.33899/edusj.2020.164375